Spatial Distribution Measurement of Molecular Activated Recombination Using Hydrogen Balmer Line Intensities of Divertor Simulation Plasma in GAMMA 10/PDX

A. Terakado[1, a)], M. Sakamoto[1], N. Ezumi[1], S. Togo[1], K. Nojiri[1], Y. Nakashima[1], K. Ichimura[1], K. Sawada[2], J. Kohagura[1]

[1] *Plasma Research Center, University of Tsukuba, 1-1-1 Tennodai, Tsukuba, Ibaraki 305-8577, Japan*
[2] *Faculty of Engineering, Shinshu University, 4-17-1 Wakasato, Nagano 380-8553, Japan*

[a)]terakado_akihiro@prc.tsukuba.ac.jp

Abstract. In GAMMA 10/PDX, spatial distribution of the occurrence of molecular activated recombination (MAR) has been studied by measuring two dimensional distributions of H_α and H_β line intensities of the divertor simulation plasma. The V-shaped target in the D-module which is installed in the west end region was exposed to the end loss plasma, and additional hydrogen gas was injected in the D-module. The electron temperature near the corner of the V-shaped target decreased to ~2 eV with increase in the neutral gas pressure in the D-module and the density roll over was observed, indicating the plasma was detached. The two dimensional distributions of the intensity ratio of H_α and H_β line intensities indicates that MAR was enhanced with increase in the neutral gas pressure and the region of the MAR occurrence spread and moved to the upstream side.

INTRODUCTION

Understanding of divertor plasma phenomena is one of the most important issues for the stable plasma operation. A divertor plate is exposed to high heat and particle fluxes [1]. Plasma detachment is indispensable for reduction of the both fluxes, and volumetric plasma recombination in the detached plasma plays an essential role in reduction of the both fluxes [2]. Radiative and three body recombination, that is electron ion recombination (EIR), is important when the electron temperature is less than about 1 eV. Another recombination process is molecular activated recombination (MAR) involving a vibrationally excited hydrogen molecule [3-8]. The rate coefficient of MAR is much greater than that of EIR at relatively high electron temperature [4]. In the MAR process, there are three chains of reaction: (1) $H_2(v) + e \rightarrow H^- + H$ followed by $H^- + H^+ \rightarrow H^+ + H^*$ (n = 2, 3), (2) $H_2(v) + H^+ \rightarrow H_2^+(v') + H$ followed by $H_2^+ + e \rightarrow H + H^*$ ($n \geq 2$) and (3) $H_2(v) + H_2^+ \rightarrow H_3^+ + H$ followed by $H_3^+ + e \rightarrow H + H + H$ and $H_3^+ + e \rightarrow H_2(v) + H^*$, where $H_2(v)$ and H* denote a vibrationally excited molecule and electrically excited atom, respectively. Balmer line emissions are enhanced by these reactions. It is important to control the plasma detachment region for stable detached plasma sustainment.

In GAMMA 10/PDX, divertor simulation experiments have been carried out using a divertor simulation experimental module (D-module) which is installed in the west-end region to study the divertor detachment and plasma-wall interaction [9-11]. Recently, detachment of hydrogen plasma has been achieved by additional hydrogen gas injection into the D-module. In this detached plasma, MAR plays a crucial role [12]. In this study, we have measured two dimensional distributions of the H_α and H_β line intensities with a high speed camera to discuss a phenomenon of MAR in the D-module.

EXPERIMENTAL SETUP

The tandem mirror GAMMA 10/PDX consists of a central cell, anchor cells, plug-barrier cells and end regions. The total length of the device is 27 m and the vacuum vessel volume is 150 m^3. The main plasma is produced and maintained by ion cyclotron range of frequency (ICRF) heating. The D-module is installed in the west-end region. Figure 1(a) shows the side view of the D-module. The V-shaped target in the D-module is exposed to the end loss plasma. Tungsten plates with the thickness of 0.2 mm are attached on the V-shaped target base. The size of the tungsten target is 0.3 m in width and 0.35 m in length. Langmuir probes are installed on the upper target and near the inlet of the D-module to measure the electron density and temperature of the plasma. Gas injection ports are set at the inlet of the D-module and the hydrogen gas is injected toward the target.

The spatial distributions of the H_α and H_β line intensities of the plasma in the D-module are measured by a high speed camera as shown in Fig. 1(b). An interference filter (656 nm ± 10 nm or 486 nm ± 10 nm) is installed in front of the camera. The both intensities were relatively calibrated by using a standard light source. In this experiment, the plenum pressure for the hydrogen gas supply was changed shot by shot to control the gas pressure in the D-module, which was measured by an ASDEX gauge installed at the top of the D-module.

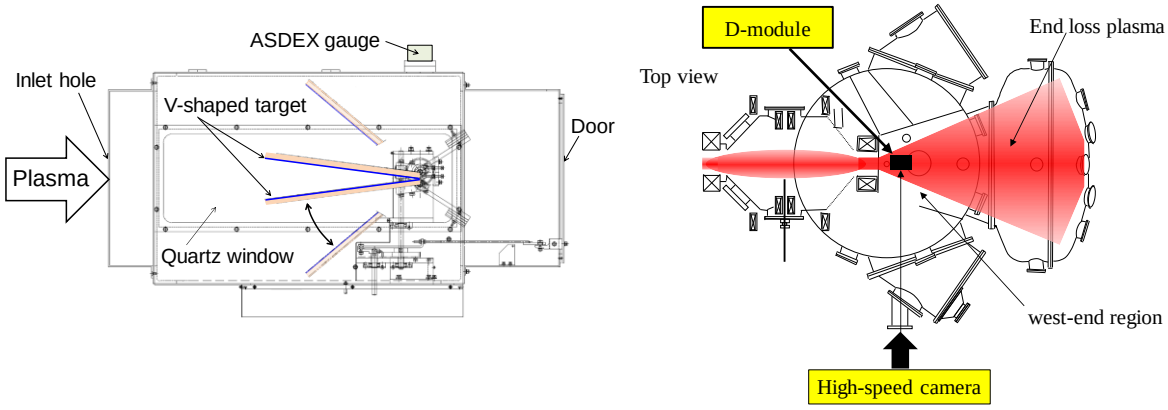

FIGURE 1. (a)Schematic views of the D-module and (b)west end region of GAMMA 10/PDX.

EXPERIMENTAL RESULTS AND DISCUSSION

The V-shaped target was exposed to the end-loss plasma for 200 ms and additional hydrogen gas was supplied in the D-module from 300 ms before the plasma production to end of the plasma. Figure 2 shows the spatial distributions of the H_α and H_β line intensities at each gas pressure, which were measured shot by shot assuming reproducibility of the plasma. The intensity was averaged over a period from 100 ms to 160 ms in which period plasma was stable. The neutral gas pressure in the D-module is shown in each image of Fig. 2. The H_α line intensity became stronger at the upstream of the plasma (i.e. left hand side of the image) with increase in the gas pressure. On the other hand, the H_β line intensity near the upstream had the maximum at the pressure of ~2 Pa and it decreased with increase in the gas pressure. The H_α and H_β line intensities near the corner of the V-shaped target decreased very much at the high neutral pressure, indicating that the plasma was detached from the target.

The electron temperature and density near the corner of the V-shaped target are also indicated at the left hand side of Fig. 2. The electron temperature decreased to ~2 eV with increasing the gas pressure. On the other hand, the electron density increased with the increase of the gas pressure up to 2 Pa and then decreased with increase in the gas pressure (i.e. density roll over), which is similar to the trend of H_β line intensity. Measurements of electron temperature and density as well as the H_α and H_β line intensities revealed that the plasma was detached through the MAR process [12].

The ratio of H_α and H_β line intensities is a good monitor for occurrence of MAR. Figures 2(i) - 2(l) show the spatial distribution of the ratio of H_α line intensity to H_β line intensity ($I_{H\alpha}/I_{H\beta}$) at each gas pressure. Figures 3(a) - 3(c) show the H_α line intensity, H_β line intensity and a ratio of those intensities as a function of z, which means a distance along the central axis from the corner of the V-shaped target. The data of Fig. 3 is extracted from the distribution of Fig. 2. Unevenness of the intensity at z ~ 130, 230 and 335 mm is caused by the reflection of edge of the flange which is installed at the opposite side of the plasma. As the gas pressure increased, $I_{H\alpha}/I_{H\beta}$ increased and the region of the

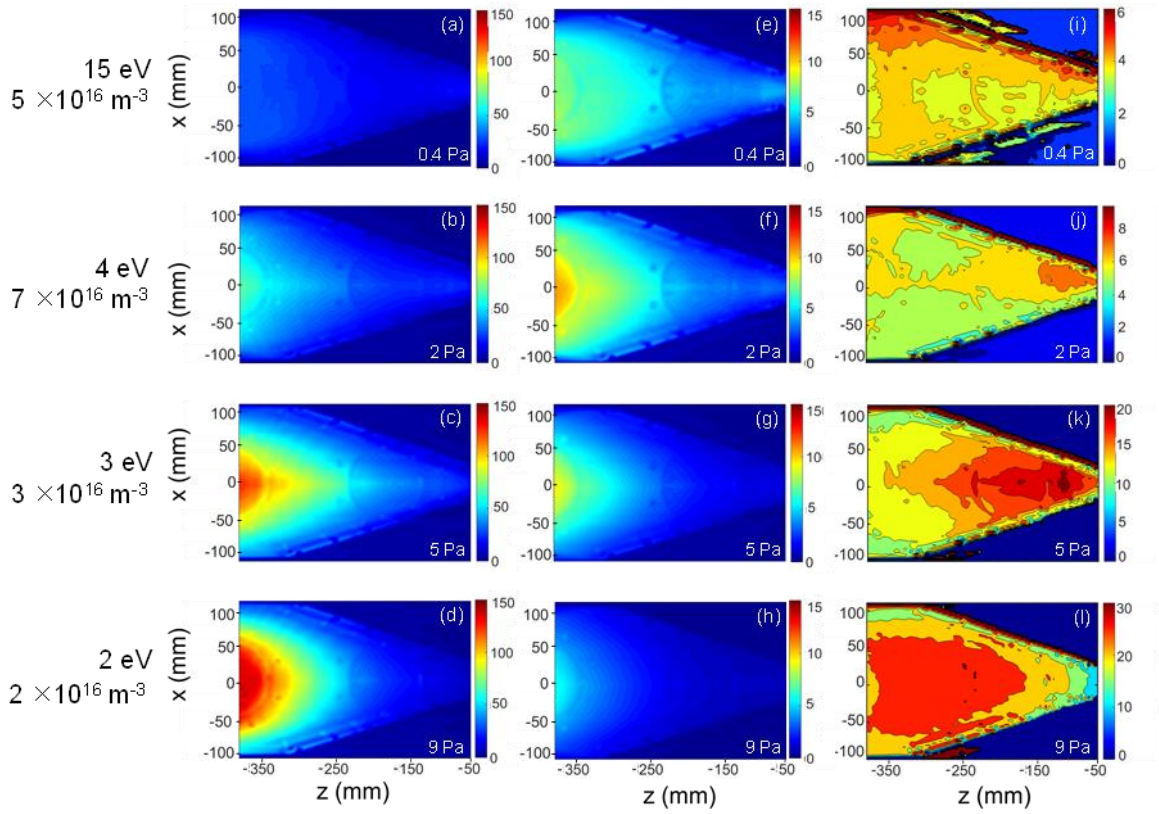

FIGURE 2. (a)-(d) Two dimensional images of H_α line intensity, (e)-(h) two dimensional images of H_β line intensity and (i)-(l) ratio of H_α intensity and H_β intensity ($I_{H\alpha}/I_{H\beta}$).

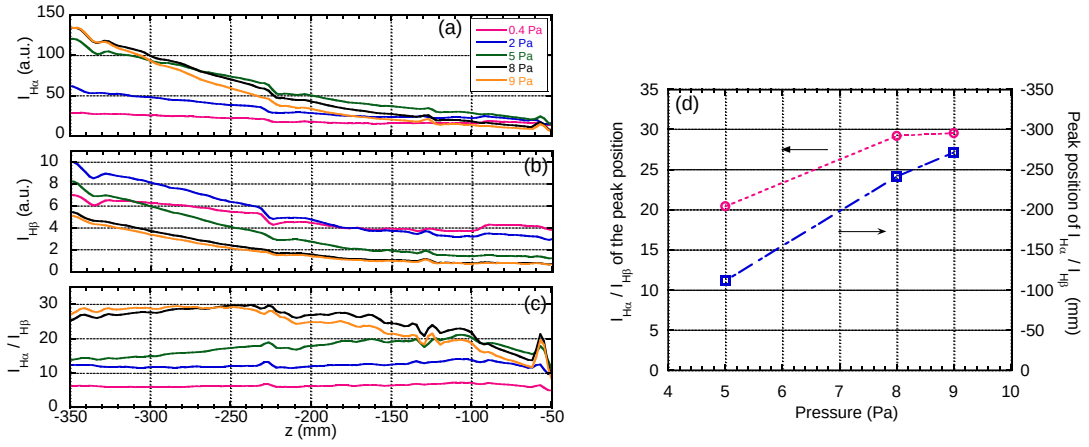

FIGURE 3. (a) H_α line intensity, (b) H_β line intensity and (c) ratio of the H_α line intensity to the H_β line intensity ($I_{H\alpha}/I_{H\beta}$) and (d) pressure dependence of the peak positon of $I_{H\alpha}/I_{H\beta}$ and $I_{H\alpha}/I_{H\beta}$ at the peak position.

high ratio moved from the corner to the upstream side and spread, indicating MAR was enhanced with increase in the neutral gas pressure and the region of the MAR occurrence spread and moved to the upstream side. The intensity ratio $I_{H\alpha}/I_{H\beta}$ increased with increase in the neutral gas pressure. The peak position of $I_{H\alpha}/I_{H\beta}$ moved to the upstream side and $I_{H\alpha}/I_{H\beta}$ became about 30 as shown in Fig. 3(d).

SUMMARY

In GAMMA 10/PDX, a divertor simulation experimental module (D-module) has been installed in the west-end region to study divertor detachment and plasma-wall interaction. The plasma was sustained by ion cyclotron heating, and the V-shaped target which was installed in the D-module was exposed to the end-loss plasma. Experiments of hydrogen gas injection to the D-module have been carried out to study spatial distribution of the MAR occurrence. The spatial distributions of H_α and H_β line intensities of the divertor simulation plasma in the D-module were measured with the high speed camera. The electron temperature near the corner of the V-shaped target decreased to ~2 eV with increase in the neutral gas pressure in the D-module and the density roll over was observed, indicating the plasma was detached. At that time, the intensity ratio $I_{H\alpha}/I_{H\beta}$ increased and the peak position of $I_{H\alpha}/I_{H\beta}$ moved to the upstream side and the area of high $I_{H\alpha}/I_{H\beta}$ spread. This indicates that MAR was enhanced with increase in the neutral gas pressure and the region of the MAR occurrence spread and moved to the upstream side, since $I_{H\alpha}/I_{H\beta}$ is a good monitor of MAR occurrence.

ACKNOWLEDGMENTS

The authors would like to thank the members of the GAMMA 10 group in University of Tsukuba for their support in the experiments. This work was performed with the support of NIFS Collaborative Research Program (NIFS13KUGM083 and NIFS16KUGM119).

REFERENCES

[1] D. Lumma, J.L. Terry, B. Lipshultz, Phys. Plasma **4,** (1997) 2555.
[2] S. I. Krasheninnikov *et al.*, Phys. Plasmas **4**, 1638 (1997).
[3] S. I. Krasheninnikov *et al.*, Phys. Lett. A **214**, 285 (1996).
[4] A. Yu. Pigarov *et al.*, Phys. Lett. A **222**, 251 (1996).
[5] N. Ohno *et al,* Phys. Rev. Lett. **81** (1998) 818.
[6] N. Ezumi *et al.,* J. Nuc. Mater. **266-269** (1999) 337.
[7] A. Tonegawa *et al.,* J. Nucl. Mater. **313-316** (2003) 1046-1051.
[8] A. Okamoto *et al.,* J. Nucl. Mater. **363-365** (2007) 395-399.
[9] Y. Nakashima, *et al.,* Trans. Fusion Sci. Technol. **63** (2013) 100.
[10] M. Sakamoto, *et al.,* Trans. Fusion Sci. Technol. **63** (2013) 188.
[11] Y. Nakashima, *et al.,* J. Nucl. Mater. **463** (2015) 537.
[12] M. Sakamoto *et al.,* 22nd International Conference on Plasma Surface Interactions in Controlled Fusion Devices, submitted to Journal of nuclear materials and energy.